Geometric phase around multiple exceptional points

Soo-Young Lee,[1] Jung-Wan Ryu,[1] Sang Wook Kim,[2] and Yunchul Chung[1,*]
[1]*Department of Physics, Pusan National University, Busan 609-735, Korea*
[2]*Department of Physics Education, Pusan National University, Busan 609-735, Korea*
(Received 2 April 2012; published 26 June 2012)

We study the geometrical phase when multiple exceptional points (EPs) are involved. In an optical microcavity of a stadium shape, we find two EPs, connected through three interacting modes, in a two-dimensional parameter space. It is shown that the geometrical phase imprinted on wave functions becomes zero when the two EPs are encircled three times in the parameter plane. In addition, we examine geometrical phases when three EPs are involved in a 3×3 matrix model, and show that single- and double-loop return modes have the geometrical phase of $\pm\pi$ or zero, depending on the type of the three EPs encircled.

DOI: 10.1103/PhysRevA.85.064103 PACS number(s): 03.65.Vf, 42.55.Sa, 05.45.Pq

Although we are familiar with Hermitian quantum systems whose energies are conserved in time, realistic quantum systems are often well described by non-Hermitian Hamiltonians [1]. In particular, when a quantum system interacts with the environment, the energy of the system can vary in time due to the energy transfer to or from the environment. In this case, the energy eigenvalue of a quantum state becomes a complex number, namely, $E_n = \omega_n \mp i\gamma_n$, where γ_n represents the energy transfer rate of the state. Recently, the non-Hermitian Hamiltonian with the so-called $\mathcal{PT}$ symmetry has attracted much attention since it can give real eigenvalues [2–4]. This suggests that we need to develop a new or generalized quantum mechanics to appropriately incorporate non-Hermitian cases [1].

Formalism for non-Hermitian systems is somewhat different from that of the standard Hermitian. First of all, there are two kinds of eigenstates, namely, the right eigenstates $|\psi_n\rangle$ and the left eigenstates $|\phi_n\rangle$, which satisfy the biorthogonality relation, $\langle\phi_m|\psi_n\rangle = \delta_{mn}$. It means, in general, $\langle\psi_m|\psi_n\rangle \neq \delta_{mn}$. This nonorthogonality has been studied and quantified by the Petermann factor [5,6] or by the phase rigidity [7]. Another important and unique feature of non-Hermitian systems is the existence of an exceptional point (EP), a degenerate point where two eigenvalues and the corresponding eigenstates coalesce [8,9]. Mathematically, the EP is a square-root-branch point. The EP is now well accepted as a real physical object since it has been revealed in numerous numerical and experimental observations in various non-Hermitian systems, such as microwave cavities [10–12], optical microcavities [6,13], and atom-cavity systems [14].

It is well known that the eigenstates acquire an additional geometrical phase $\pm\pi$ after a double-cyclic parameter variation encircling an EP. In a microwave experiment with coupled asymmetric cavities, Dembowski *et al.* [10] have found the geometrical phase $\pm\pi$ for a double-cyclic loop by measuring the variation of intensity pattern of eigenstates, and Dietz *et al.* [11] have shown, by using an improved technique, that geometric amplitude is different from unity when time-reversal invariance is violated. Recently, it has been shown that the geometrical phase associated with an EP can be extracted from wave functions by tracing their continuous phase variation [15].

In this Brief Report, we study the geometrical phase when multiple EPs are involved. Eigenvalue surface structures around two or three EPs have been recently demonstrated in coupled optical microcavities and a simple 3×3 matrix model [16]. It is interesting to examine the geometrical phase for such systems, which is shown to be quite nontrivial. First, we find two EPs associated with three interacting modes (see Fig. 1) in a stadium-shaped microcavity. We demonstrate that the geometrical phase becomes zero when two EPs are encircled three times in a parameter plane. This can be understood by a direct addition of two partial geometrical phases $\pm\pi$ generated from each individual EP. From the eigenvalue structure of the 3×3 matrix model (e.g., see Fig. 4), it has been found that three eigenstates can be split into two groups: one state returns to itself after parametric variation along the loop encircling three EPs once, called a single-loop return mode (SRLM), while two states return to themselves after parametric variation twice, called a double-loop return mode (DLRM). We show that SLRM and DLRM exhibit the geometric phase of $\pm\pi$ or zero, depending on the type of three EPs that are encircled.

In general, a wave function, obtained from an eigenvalue equation, has an arbitrary overall phase. Therefore, one might think that the wave functions, due to the arbitrary phase factor, are useless for finding the geometrical phase. However, it has been shown that there exist two ways to extract the geometric phase from the wave functions: during the parametric variation by continuously tracing (i) the complex inner product of an eigenstate and (ii) the phase distribution of an eigenstate in coordinate space, called a phase plot [15]. In this Brief Report, we will exploit the phase-plot method to calculate the geometrical phase.

In the phase-plot method, we fix the overall phase by requiring the inner product $\langle\psi_n^*|\psi_n\rangle$ defined as $\langle\psi_n^*|\psi_n\rangle = \int d\mathbf{x}\,\psi_n(\mathbf{x})^2$, where the integration is performed only inside the microcavity, to be positive in order to remove the phase arbitrariness mentioned above [17]. Then, the geometrical phase γ_B appears as the phase difference between the initial $|\psi_n\rangle_I$ and final states $|\psi_n\rangle_F$ of a given cyclic parameter variation:

$$|\psi_n\rangle_F = \exp(i\gamma_B)|\psi_n\rangle_I. \tag{1}$$

Considering the wave function in the polar form

$$\psi_n(\mathbf{x}) = r(\mathbf{x})e^{i\theta(\mathbf{x})}, \tag{2}$$

*ycchung@pusan.ac.kr

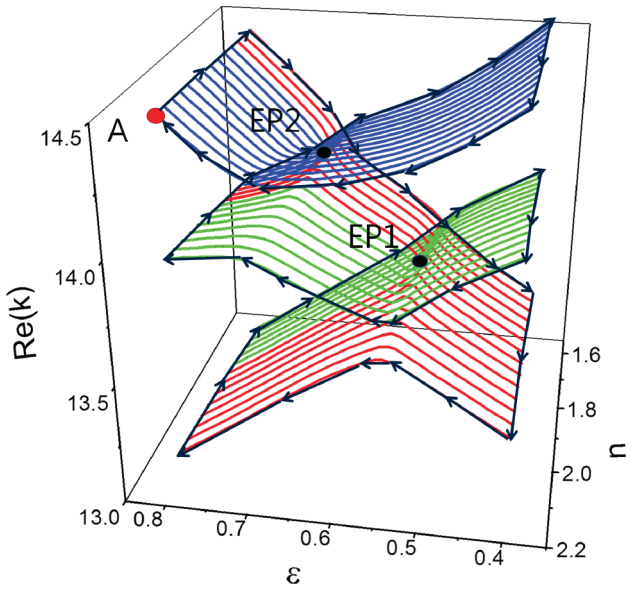

FIG. 1. (Color online) The structure of the real eigenvalue of a stadium-shaped optical microcavity as a function of ε and n, when two EPs are connected through three interacting modes.

where $\theta(\mathbf{x})$ is a phase function and $\mathbf{x}$ represents a two-dimensional vector in coordinate space, γ_B is determined by the difference between the initial and final phase function, $\gamma_B = \theta_F(\mathbf{x}) - \theta_I(\mathbf{x})$, which must be $m\pi$ with an integer m irrespective of $\mathbf{x}$.

In a stadium-shaped optical microcavity, by using the boundary element method [18], we calculate the complex wave numbers k of resonance modes to find two EPs, associated with three interacting modes, in the parameter plane (ε,n), where ε is the length of the straight part divided by the diameter of the half circle of the stadium billiard, and n is the refractive index. The EPs are located at $(\varepsilon_{EP1},n_{EP1}) = (0.54,1.89)$ and $(\varepsilon_{EP2},n_{EP2}) = (0.68,1.70)$, whose corresponding degenerated wave numbers or eigenvalues are $k_{EP1} = 13.66 - i0.45$ and $k_{EP2} = 14.01 - i0.57$, respectively. Figure 1 shows how the real part of the eigenvalue k evolves to form a surface structure as ε and n vary encircling two EPs three times. Note that there exist three modes at a given (ε,n). As guided by arrows, it is easily seen that each mode comes back to itself after three-cyclic variations encircling both EPs, which has been discussed in Ref. [16].

The eigenvalue surface can be understood as a simple connection of two square-root-branch structures that is observed in the single-EP case [6,9]. This connection is well demonstrated by traces of eigenvalues on the complex eigenvalue plane, as shown in Fig. 2. Here we consider two straight lines in the (ε,n) plane, with one passing just above two EPs and the other passing just below two EPs [see the black and red lines in Fig. 2(a)]. For the parameter changes along these two lines, we trace complex eigenvalues of three interacting modes, and the results are presented in Fig. 2(b). It is clearly seen that two local characteristic structures of an EP are simply connected in the complex eigenvalue plane.

In order to get the geometrical phase, we have to trace the continuous change of phase function $\theta(\mathbf{x})$ induced by a cyclic parameter variation encircling the two EPs. Here we consider

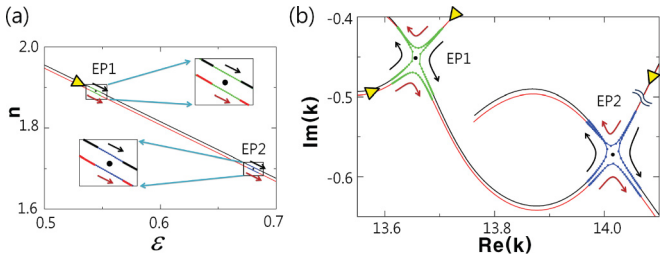

FIG. 2. (Color online) (a) Two lines passing slightly above and below two EPs in the parameter plane (ε,n). (b) Traces of three eigenvalues in a complex plane when parameters are varied along the two lines in (a). Three yellow triangles indicate the eigenvalues of three interacting modes at the parameter marked by the yellow triangle near EP1 in (a).

the parametric variation along a rectangular path in the (ε,n) plane, namely, $(0.4,1.6) \rightarrow (0.8,1.6) \rightarrow (0.8,2.0) \rightarrow (0.4,2.0) \rightarrow (0.4,1.6)$. During the parametric variation, the change of phase $\theta(\mathbf{x})$ of an eigenstate can be obtained by tracing the phase at a certain specific position $\theta(\mathbf{x}_p)$ instead of looking at the whole $\theta(\mathbf{x})$. This is because the geometrical phase γ_B is not a function of $\mathbf{x}$. In Fig. 3(a), we present how the phase at a specific position $\mathbf{x}_p = (0.7R,0.7R)$, with the radius R of the half circle of the stadium, varies as the parameters cyclically evolve along the rectangular path mentioned above. After three-cyclic variations encircling both EPs, the resulting phase difference is 2π, as indicated by the blue line. This means that one cannot obtain a nontrivial geometrical phase

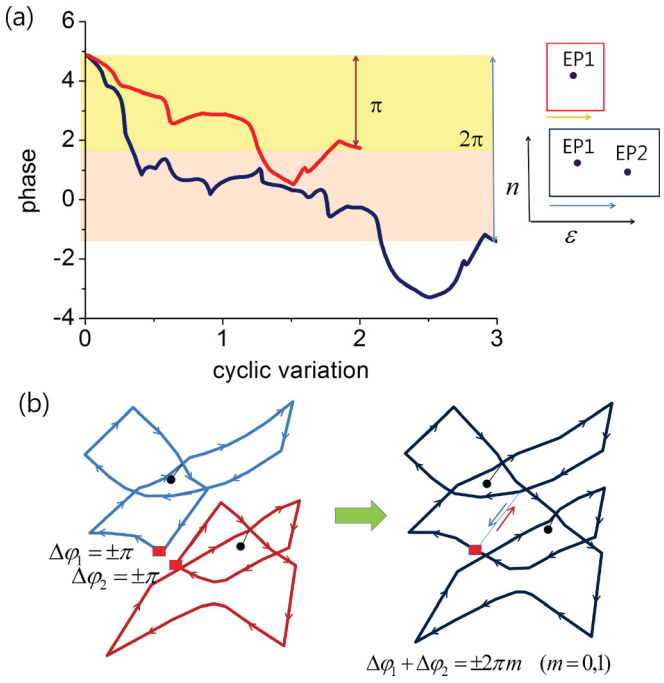

FIG. 3. (Color online) (a) Phase evolution at $\mathbf{x}_p$ inside the stadium-shaped microcavity. The upper red line shows the geometrical phase π after double-cyclic variations encircling EP1, and the lower blue line shows 2π after three-cyclic variations encircling both EP1 and EP2. How the cyclic variations are performed are shown in the right panel. (b) Conceptual explanation of the trivial geometrical phase in the two-EP case.

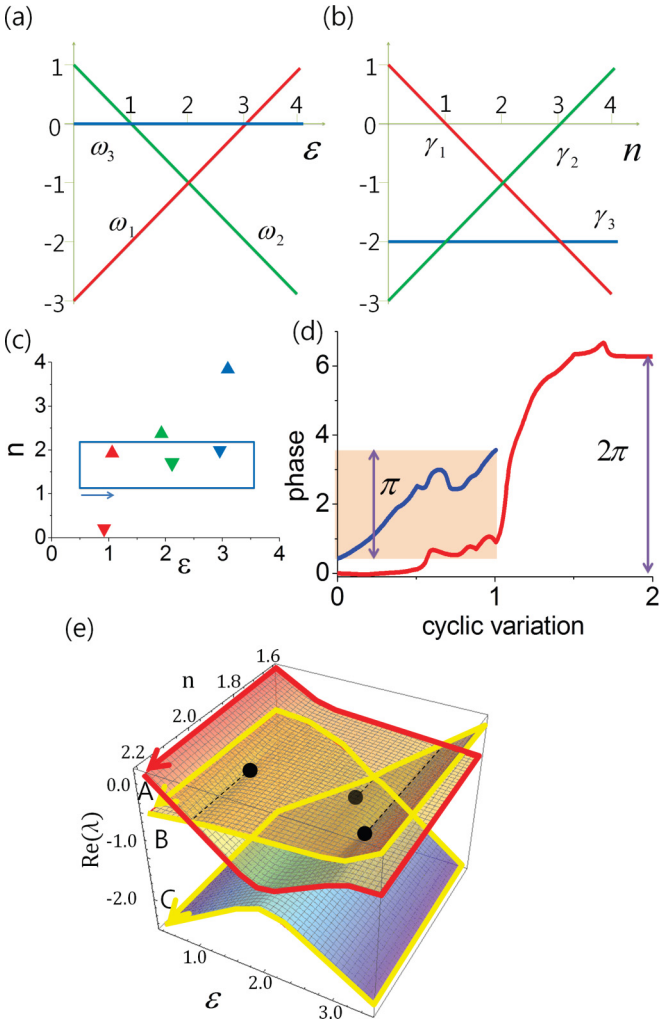

FIG. 4. (Color online) The (a) real and (b) imaginary part of energies E_m of the diagonal components of the 3×3 matrix as a function of ε and n, respectively. (c) Triangles represent six EPs obtained from the matrix model. The square denotes the loop considered here. (d) The blue and the red curves show the phase evolution of the SLRM and the DLRM, respectively. (e) The evolution of the real eigenvalues as the parametric variation is performed along the loop of (c); the SLRM (DLRM) follows the red (yellow) curve.

in the two-EP case, unlike the $\pm\pi$ phase change in the one-EP case (see the red line). It can be easily understood by considering a schematic diagram, shown in Fig. 3(b). First consider two individual EPs, each of which exhibits $\Delta\varphi_{1,2} = \pm\pi$ phase change after a double-cyclic variation encircling each EP [10,15]. Let us now combine these two eigenvalue surfaces. The phase changes along the combined line are exactly canceled out, giving rise to a single eigenvalue surface of a three-cyclic variation. The total phase change is then given by the sum of individual phase changes, i.e., $\Delta\varphi_1 + \Delta\varphi_2 = \pm 2\pi$ or 0.

Let us move to the three-EP case. We will use a 3×3 matrix model inspired by interacting modes of the optical microcavity, which is proposed in Ref. [16], since it is difficult to find three EPs associated with three interacting modes in the stadium-shaped microcavity. It is known that when two resonance modes of energies $E_1 = \omega_1 - i\gamma_1$ and $E_2 = \omega_2 - i\gamma_2$ interact with each other with the coupling strength δ, the EP takes place at $\delta = |\gamma_1 - \gamma_2|/2$ with $\omega_1 = \omega_2$ [13]. By extending this simple model, we can make a 3×3 matrix model which allows us to estimate where EPs occur. The diagonal elements of the model Hamiltonian are given as $E_m = \omega_m - i\gamma_m$ ($m = 1,2,3$), and all off-diagonal elements are set identically as a coupling strength δ which is real. Now we assume that ω_m and γ_m depend only on ε and n, respectively, i.e., $\omega_m(\epsilon)$ and $\gamma_m(n)$.

For simplicity, we regard the parametric dependence of both ω_m and γ_m to be linear, as illustrated in Figs. 4(a) and 4(b). Note that the modes 2 and 3 cross at $\mu_{23} = (\varepsilon_{23}, n_{23}) = (1,1)$, the modes 1 and 2 cross at $\mu_{12} = (\varepsilon_{12}, n_{12}) = (2,2)$, and the modes 1 and 3 cross at $\mu_{13} = (\varepsilon_{13}, n_{13}) = (3,3)$. When a small nonzero coupling δ is introduced, two EPs appear around each crossing point μ_{ml}, giving six EPs in total. The reason is that near the crossing point, there are two points satisfying the condition that the EP occurs; for example, two points $(\varepsilon_{23}, n_\pm)$, where $n_\pm = n_{23} \pm 2\delta$, satisfy the condition $\delta = |\gamma_2 - \gamma_3|/2$. As δ increases, the distance between the two EPs would increase to show some deviation from the single-EP estimation, due to the influence of the third mode. For $\delta = 0.4$, six EPs are shown in Fig. 4(c). The red triangles at $\varepsilon \sim 1$ represent the EPs of modes 2 and 3. The upward and downward triangles are denoted by $EP_{23,U}$ and $EP_{23,D}$. The green triangles at $\varepsilon \sim 2$ ($EP_{12,U}$ and $EP_{12,D}$) and the blue triangles at $\varepsilon \sim 3$ ($EP_{13,U}$ and $EP_{13,D}$) are assigned in a similar way. Note that the energy surface structure near these paired EPs, e.g., $EP_{12,U}$ and $EP_{12,D}$, is different from that of the previous two EPs of the stadium microcavity because the former arises from the interaction between two modes, while the latter arises from the three-mode interaction. In fact, no nontrivial geometric phase takes place if paired EPs are encircled [19]. This can be understood by considering the case of $\delta = 0$, where the modes are independent so that the geometrical phase is zero. Encircling the paired EPs for $\delta \neq 0$ is topologically equivalent to the $\delta = 0$ case.

To examine the nontrivial case of encircling three EPs, we choose only one from each paired EP so that the loop encircles three EPs coming from three different paired EPs, as shown in Fig. 4(c) where the encircled EPs are $EP_{23,U}$, $EP_{12,D}$, and $EP_{13,D}$. The structure of the real energy surface is presented in Fig. 4(e) [16]. It is clearly seen that one mode among three interacting modes comes back to itself after a single-cyclic variation encircling the three EPs (SLRM, see the red guide arrow), while the remaining two modes return back to themselves by double-cyclic variation (DLRM, see the yellow guide lines). Here, we examine the geometrical phase for both the SLRM and DLRM by using the phase-plot method. The procedure is the same as before. First, we determine the arbitrary phase of an eigenvector $\mathbf{v} = (v_1, v_2, v_3)$ in a way that the inner product $\mathbf{v} \cdot \mathbf{v} = v_1^2 + v_2^2 + v_3^2$ becomes a real positive value. Then, we trace the phase of the first component v_1 as the parameters vary along the loop. The phase changes are shown in Fig. 4(d). The SLRM shows π difference while the DLRM shows 2π. However, this is not a unique phase difference for three-EP cases.

When we choose a loop including different combination of EPs, e.g., by encircling $EP_{13,U}$ instead of $EP_{13,D}$ as shown

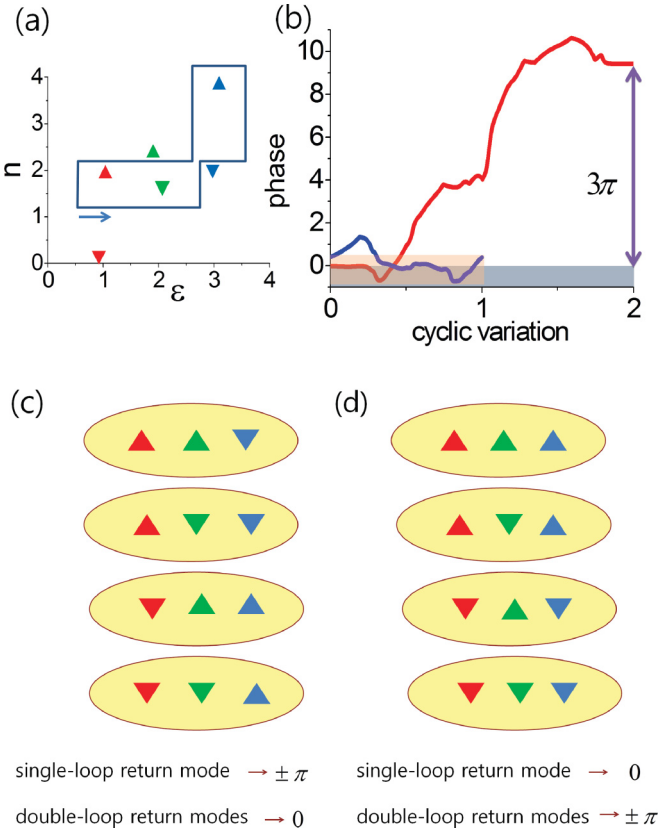

FIG. 5. (Color online) (a), (b) The same as Figs. 4(c) and 4(d) with a different loop encircling three different EPs. (c) The class exhibiting $\gamma_B = \pm(2m+1)\pi$ for SLRM and zero for DLRM. (d) The class exhibiting $\gamma_B = \pm(2m+1)\pi$ for DLRM and zero for SLRM.

in Fig. 5(a), the result become exactly opposite; the SLRM gives rise to zero phase difference, while 3π is the result for DLRM, as illustrated in Fig. 5(b). All of the three-EP cases fall into these two classes, as summarized in Figs. 5(c) and 5(d). It is interesting to point out that the type (up and down) of the central EP, EP_{12}, does not play any role in determining the class. When the type of the side EPs is different, the SLRM shows the nontrivial geometrical phase $\gamma_B = \pm(2m+1)\pi$, where m is an integer. On the contrary, when the side EPs belong to the same type, the DLRM shows the nontrivial geometrical phase.

It might be interesting to note that both the geometrical phases of the two-EP case in the microcavity and the nontrivial single-loop case of Fig. 5(a) are equivalent to those of the triple-degeneracy point [20,21]. This might imply that both cases can continuously contract to form the triple-degeneracy point.

In summary, we have studied the geometrical phase arising when two EPs or three EPs are encircled in a parameter plane. Based on numerical calculations for a stadium-shaped optical microcavity, we have shown that the two-EP case is trivial, i.e., zero geometrical phase. On the other hand, for the three-EP case, we found, using a 3×3 matrix model, that the behavior of the geometric phase is categorized into two classes depending on what kind of EPs are encircled.

S.Y.L. was supported by NRF Grant No. 2010-0008669. S.W.K. was supported by the NRF grant funded by the Korea government (MEST) (Grants No. 2009-0084606 and No. 2010-0024644). Y.C. was partially supported by the NRF grant funded by the MEST (Grant No. 2011-0003109) and the KOSEF grant funded by the MEST (Grant No. 2010-0000268).

[1] N. Moiseyev, *Non-Hermitian Quantum Mechanics* (Cambridge University Press, New York, 2011).
[2] C. M. Bender and S. Boettcher, Phys. Rev. Lett. **80**, 5243 (1998).
[3] A. Guo, G. J. Salamo, D. Duchesne, R. Morandotti, M. Volatier-Ravat, V. Aimez, G. A. Siviloglou, and D. N. Christodoulides, Phys. Rev. Lett. **103**, 093902 (2009).
[4] C. E. Rüter, K. G. Makris, R. El-Ganainy, D. N. Christodoulides, M. Segev, and D. Kip, Nature Phys. **6**, 192 (2010).
[5] K. Petermann, IEEE J. Quantum Electron. **15**, 566 (1979).
[6] S.-Y. Lee, J.-W. Ryu, J.-B. Shim, S.-B. Lee, S. W. Kim, and K. An, Phys. Rev. A **78**, 015805 (2008).
[7] E. N. Bulgakov, I. Rotter, and A. F. Sadreev, Phys. Rev. E **74**, 056204 (2006).
[8] T. Kato, *Perturbation Theory for Linear Operators* (Springer, Berlin, 1966).
[9] W. D. Heiss, Phys. Rev. E **61**, 929 (2000).
[10] C. Dembowski, H.-D. Gräf, H. L. Harney, A. Heine, W. D. Heiss, H. Rehfeld, and A. Richter, Phys. Rev. Lett. **86**, 787 (2001).
[11] B. Dietz, H. L. Harney, O. N. Kirillov, M. Miski-Oglu, A. Richter, and F. Schäfer, Phys. Rev. Lett. **106**, 150403 (2011).
[12] S. Bittner, B. Dietz, U. Günther, H. L. Harney, M. Miski-Oglu, A. Richter, and F. Schäfer, Phys. Rev. Lett. **108**, 024101 (2012).
[13] S.-B. Lee, J. Yang, S. Moon, S.-Y. Lee, J.-B. Shim, S. W. Kim, J.-H. Lee, and K. An, Phys. Rev. Lett. **103**, 134101 (2009).
[14] Y. Choi, S. Kang, S. Lim, W. Kim, J.-R. Kim, J.-H. Lee, and K. An, Phys. Rev. Lett. **104**, 153601 (2010).
[15] S.-Y. Lee, Phys. Rev. A **82**, 064101 (2010).
[16] J.-W. Ryu, S.-Y. Lee, and S. W. Kim, Phys. Rev. A **85**, 042101 (2012).
[17] S.-Y. Lee, Phys. Rev. A **80**, 042104 (2009).
[18] J. Wiersig, J. Opt. A: Pure Appl. Opt. **5**, 53 (2003).
[19] F. Keck, H. J. Korsch, and S. Mossmann, J. Phys. A: Math. Gen. **36**, 2125 (2003).
[20] W. D. Heiss, J. Phys. A: Math. Theor. **41**, 244010 (2008).
[21] G. Demange and E.-M. Graefe, J. Phys. A: Math. Theor. **45**, 025303 (2012).